This is a draft version to be updated at a regular basis

Current update is from June 8, 2022

Instrumental Features Near the Si K Edge in the CHANDRA HETG 1st Order

Norbert S. Schulz,[1] with the Chandra HETG/ACIS Calibration Teams,[1],[2],[3]

1. Introduction

There have been several studies of the Si K edge absorption and edge structure in the past decade which produced a large amount of data and detailed information about the shape of the edge. These studies all use the high energy transmission grating spectrometer (HETGS), which consists of the high energy transmission gratings (HETG) and the Advanced CCD Imaging Spectrometer (ACIS) array ACIS-S.

In a first comprehensive survey Schulz et al, (2016) used Chandra HETG archive data to characterize Si K edge absorption in 11 very bright low-mass X-ray binaries (LMXBs). There it was concluded that most of the data were insuffiecent for two major reasons. One was that data taken in timed event mode (TE) were riddled with photon pile-up, the other one was that data taken in continuous clocking mode, which are generally pile-up free, smear the data to the extent that it affects spectral resolution.

Zeegers et al (2017) applied laboratory measurements of silicate absorption to data of GX 5-1 taken in alternate exposure mode, which severely reduces CCD frametime and avoids the pile-up problem. However that study did not focus on the detailed Si K edge structure.

There was some ground calibration of the Si K transmission function in CCD devices at various synchrotron facilities. There were extensive calibration activities at the X-Ray Calibration Facility (XRCF), which mainly focussed on the HETG 1st orders, but not specific to the Si K edge region. On-orbit calibration of the HETG 1st orders were also carried out early in the mission and resulted in a slight adjustement of the high energy grating (HEG) 1st orders with respect to the medium energy grating (MEG) 1st orders (Marshall et al. 2012). However, effective area near the Si K edge again was never verified on-orbit at high resolution. In this document we want to bring attention to issues that were discovered while studying the Si K edge and its structure in bright X-rau sources

[1]Kavli Institute for Astrophysics and Space Research, Massachusetts Institute of Technology, Cambridge, MA 02139.

[2]Center for Astrophysics, Cambridge, MA 02139.

[3]Marshall Space Flight Center, Huntsville, AL.

2. Observations

Table 1 lists all the observations involved in this calibration analysis. One of the guiding principles in choosing these targets was that there was no line emissions expected and count rates were below 0.01 cts/s/pix[frametime]. The latter guarantees that emissions do not suffer from CCD pileup in the HETG spectra. For the pixel value we averaged over the 3x3 event detection island over a 2 - 7 Åbandpass and the standard extraction cross-dispersion. The cts/s/pix[frametime] is thus an average of the entire extracted HEG 1st order. For all sources, except for PKS 2155-304, the spectral slope increases towards higher energies and the cts/s/pix[frametime] value at Si K is lower than the value listed in Table 1. For PKS 2155-304 the slope increases towards lower energies and the value is somewhat lower than what is expected at Si K, but not significantly. All these values are low enough to ensure that there is no pileup at Si K in all the spectra.

For this to happen two conditions had to be applied. The sources either have to be very bright requiring a pileup mitigation setup to reduce frame time. Or the sources are faint enough for full frame operation but with sufficiently long exposures. For the latter we have two sources in the sample, PKS 2155-304 for 153 ks and Mkn 421 for 117 ks. These are ideal targets as at column densities of the order of 10^{20} cm^{-2} there are no Si K absorptions to be expected. However we also want to inspect sources where column densities are high enough to observe Si K edge structure unrelated to instrumental effects, i.e. significantly above 10^{21} cm^{-2}. Here for sources below 250 mCrab we applied a 350 row subarray with 4 CCDs on and HEG +/- 1st orders co-added, for brighter sources we applied a 134 row subarray with 2 CCDs on and only the HEG -1st order registered.

TABLE 1 CALIBRATION SOURCE PROPERTIES

Sources	Obsids	exposure (1)	Cts/s (2)	frametime (3)	Cts/s/pix[frametime] (4)
GX 5-1	19449, 20119	92.6	29.5	0.38	3.76
GX 3+1	16307, 16492, 18614 19890, 19907, 19957 19958	213.6	22,9	0.80	6.14
GX 13+1	2708, 11814, 11815 11816, 11817	113.6	13,6	0.80	3,65
GX 340+0	18065, 19450, 20099	144,9	16.9	0.38	2.15
GX 349+2	13220, 18084	39.3	35.3	0.59	7.56
Ser X-1	17485, 17600	120.3	22.0	0.38	2.80
4U 1705-44	18086, 19451, 20082	131.4	8.2	0.38	1.04
4U 1728-34	19452, 20106, 20107	110.9	2.9	0.38	0.37
4U 1636-53	20791, 21099, 21100	127.9	4.4	0.80	1.18
Mkn 421	10663, 10670, 13098 13105, 14320, 15477 15484	117.0	4.4	2.40	3.41
PKS 2155-304	337, 1014, 1795 3167, 3706, 3708 5173, 6926, 7291 8380, 8436, 9705 9712	153.4	0.65	3.21	4.37

(1) in ks for all listed obsids, (2) 3x3 pix average, (3) in s, (4) in units of 10^{-3}

All cases require large exposures. Full frame observations because the sources are faint, subarray bright sources because not all grating arms are available. The optimal setup for observing detained Si K structures is the 350 row setup because here both HEG dispersions are recorded at long exposures.

3. Si K Edge in HETG Observations

In the following we present Si K edge bandpass emissions for low and higher NH cases. We mostly use HEG data as here we have the maximum spectral resolution in 1st order.

3.1. Low NH Case

At column densities well below 10^{21} cm^{-2} we do not expect any Si K absorption edge structures other than what is provided by the ACIS instrument. Idealy when the effective area of the ACIS-S CCDs is removed the HEG spectrum should not show any structure related a Si K edge. Figure 1 on the left shows four residual spectra of low NH X-rays sources as presented by Rogantini et al. 2020. It involves three LMXB and one quasar source. In all cases the authors detected very similar line emissions (red line) at a wavelength of 6.742 Åindepended of source column density and source flux. Furthermore they found that the relative line flux with respect to the underlying contiuum was the same within statistical uncertainties from which it was concluded that this is an instrumental feature.

The average cts/s/pix[frametime] in the three LMXBs using TE mode data is close to 0.01 so we avoided these data. We selected the Mkn 421 and another quasar source PKS 2155-304 from the archive to investigate this line emission further. The right part or Fig. 1 shows the Si K region for these two sources. In both cases we detect the line emission at 6.742 Åabove the 3 σ level. In addition we also detect a second emission line at 6.714 Åof apparantly similar strength. This is peculiar as we also see this emission in the Rognatini et al. 2020 plot, however there this emission was ignored.

The plots in Fig. 1 to the right show three panels for PKS 2155-304 on top and three panel for Mkn 421 at the bottom. The top panel for each source shows the raw HEG co-added first orders at Si K. The middle panel shows the same but now including the MEG 1 orders binned on the raw MEG grid. The importance of this plot is that is shows these line missions are less obvious at higher binning. This spectrum includes the MEG +/- 1st orders and is binned to the raw MEG grid, which is twice the size of the raw HEG grid and also includes the MEG +1st order. This order has the largest effective area of the four grating arms and here the Si K edge falls on the back-illuminated CCD S3. We do not detect any excess emission in that order. The bottom plot in each set then shows the HEG broadband spectra binned to the resolution element showing now obvious issues at the Si K region beyond statistical fluctuations.

The emission at 6.742 Å is marked with a red dotted line in Figure 1. We also detect the second line above the 3 σ level and it is marked by a blue dotted line in all plots. We then fitted the local spectrum around the Si K edge with a powerlaw and two Gaussian functions. That result is seen in Figure 2. Mkn 421 seems to have an intrinsic warm absorber, which we ignore in the fit because it does not significantly interfere with the line fits. Table 2 shows the line properties. The line fluxes at 6.714 Å and 6.742 Å are very similar for each source and their flux ratio is close to unity within statistical uncertainties. Listed are also the flux ratios with the continuum, which are again similar for the two sources within

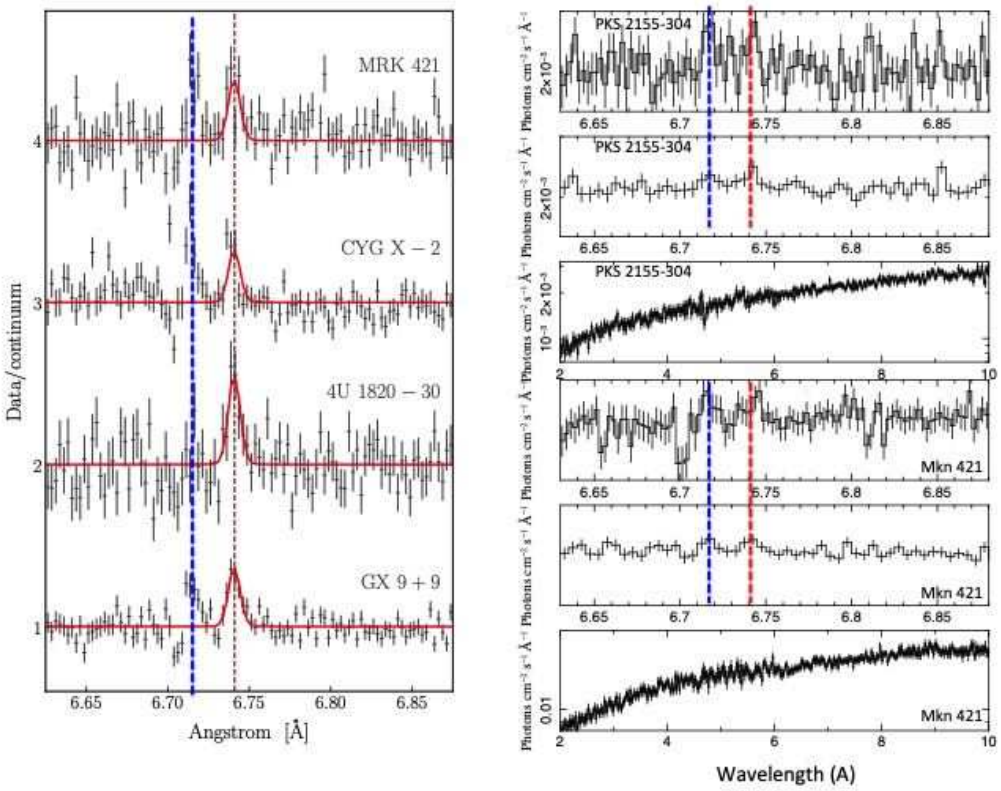

Fig. 1.— *Left:* The Si K edge in HEG data of low NH sources from Rogentini et al. 2020. The data were divided by the continuum and then stacked into the four positions for plotting purpose. The model (red) includes the source continuum and an emission line at 6.742 Å(red dotted line). A second line at 6.714 Å(blue dotted line) was not recognized at the time. *Right:* Data of the Si K edge region for PKS 2155-304 (top three plots) and Mkn 421 (botton three plots). For each source the top panel shows combined HEG 1st orders unbinned. The middle panel shows HEG 1st and MEG 1st combinded, The bottom panel shows the broadband continuum for the combined HEG 1st orders binned to a resolution element of 0.011 Å.

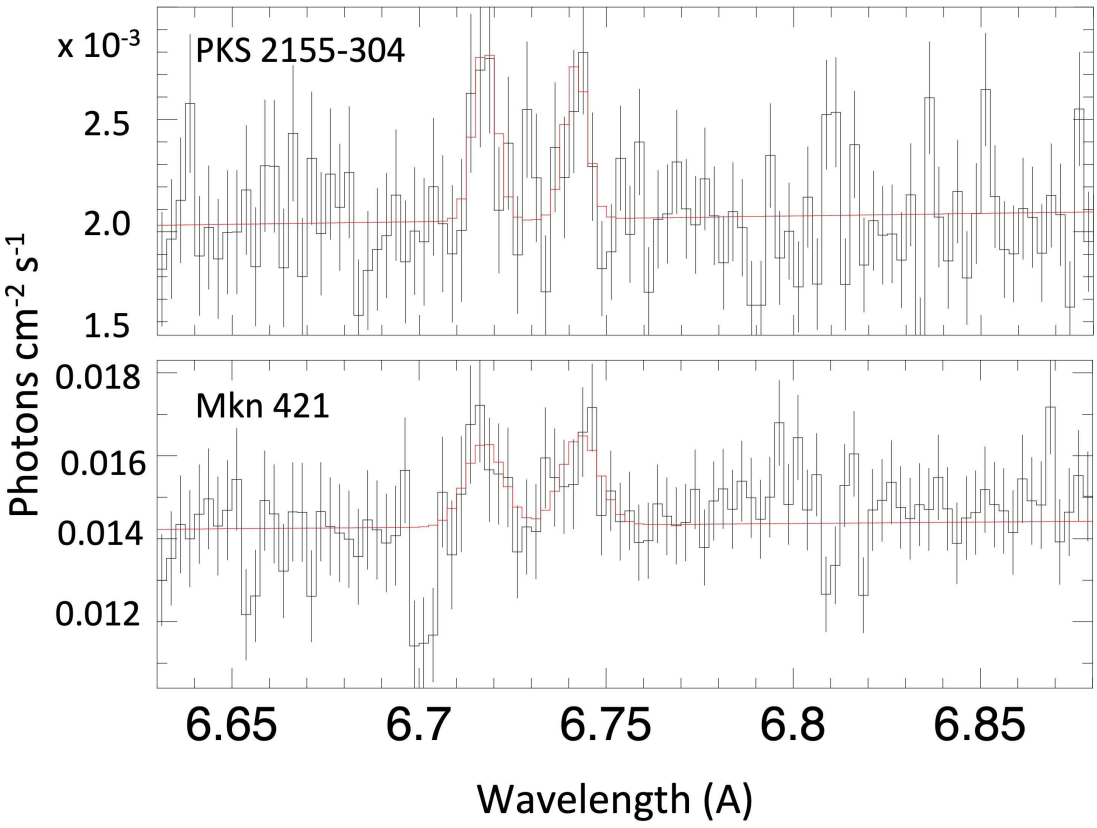

Fig. 2.— Fit of the Si K edge region in HEG data of low NH sources. *Top:* Fit of the Si K edge region in HEG data of PKS 2155-304. *Bottom:* Fit of the Si K edge region in HEG data of Mkn 421.

statistical uncertainties. The R_{line} line values are the ratios between the emission at 6.742 Å to the one at 6.714 Å.

TABLE 2 Si K EMISSION LINE PROPERTIES

Sources	N_h (1)	Wavelength [Å]	F_{line} (2)	F_{line}/F_{cont} (3)	R_{line} (4)
PKS 2155-304	0.2	6.742±0.003	0.54±0.30	2.6±1.4	
		6.717±0.002	0.63±0.37	3.0±1.8	0.86±0.81
MKN 421	0.3	6.742±0.004	2.80±1.35	1.9±0.9	
		6.718±0.004	2.64±1.68	1.9±1.2	1.06±0.80
Ser X-1	10.2	6.738±0.002	30.7±10.3	3.1±1.0	
		6.716±0.004	44.2±11.9	4.3±1.2	0.69±0.43
GX 3+1	31.3	6.742±0.001	40.3±22.2	6.7±3.7	
		6.717±0.001	44.8±23.1	7.5±3.9	0.90±0.75

(1) 10^{21} cm^{-2}; (2) 10^{-5} ph cm^{-2} s^{-1};
(3) $10^{-}3$; (4) $F_{6.74}/F_{6.71}$

3.2. High NH Case

There are no very bright sources in the *Chandra* archive with low columns and in ACIS TE mode, simply because the event mode in these cases is generally set to ACIS CC mode. The latter mode is not useful to study the Si K edge structure with the HETG spectrometer (Schulz et al. 2016). TE mode data for very bright sources have been provided so far exclusively for high absorption studies. Here we also looked at two sources with high columns, Ser X-1 and GX 3+1. The analysis gets more difficult as the Si K edge structure becomes significant and complex. Schulz et al (2016) proposed that there are two edges to be expected, an edge attributed to the ISM gas phase at 1.839 keV (6.742 Å) and another edge attributed to silicate dust at 1.844 keV (6.724 Å). That study also tentatively suggested that line emissions at 6.742 Åcould possibly be due to ISM scattering. Current scattering models have ruled that out since then. We applied a model consisting of a gas edge function at 6.742 Åand a silicate edge at 6.724 Åplus the two Gaussian emission line functions identified at low NH, which coincidently are located right on top of these edges. We for now ignore other effects such as ionized Si K absorption, which is treated in Yang et al. 2022. We see the two line emissions at 6.742 Åand 6.717 Åin both model fits. The fit results are shown in Figure 3, line properties are summerized at the bottom of in Table 2. Even though the

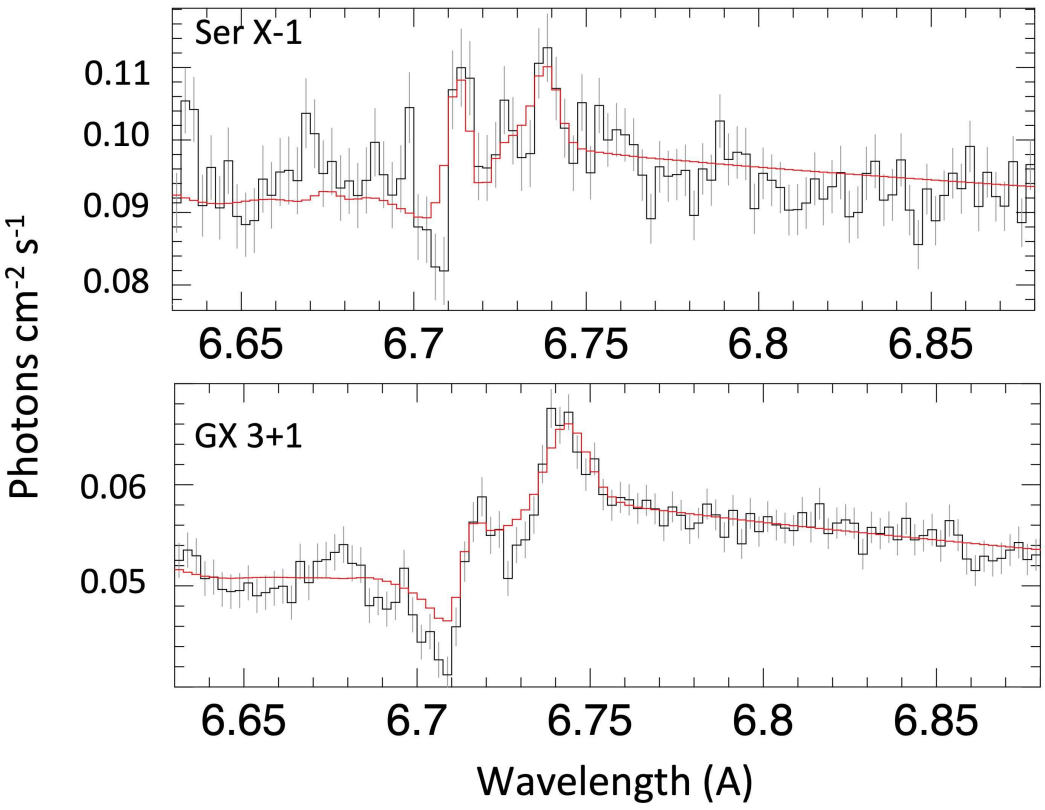

Fig. 3.— Fit of the Si K edge region in HEG data of high NH sources. *Top:* Fit of the Si K edge region in HEG data of Ser X-1. *Bottom:* Fit of the Si K edge region in HEG data of GX 3+1.

edge fits are more complex, we identify similar properties of these line emissions. Though the line to continuum ratios trend to be higher in the brighter sources, they are still similar within 90% uncertainties. The R_{line} ratios also are consistent with unity as observed in the low N_h case.

A Si K edge survey of bright LMXBs towards the Galactic Bulge conducted by Yang et al, 2022 includes nine bright LMXB between column densities of $4{\times}10^{21}$ cm^{-2} and $9{\times}10^{22}$ cm^{-2}. They applied a fully developed model consistent of a gas edge, silicate edge function and ionized Si absorption. The two Gaussion emission lines at 6.742 Åand 6.717 Åwith the constraint that these line fluxes match within 10% and 40% depending on statistics. Figure 4 middle and right panel show the properties of the edge structure fits with respect to these emission lines. The right plot shows the R_{line} ratios for the smaple and even though there is some scatter likely caused by the complexity of the fits, they are still consistent with unity.

The middle plot shows the location of the emission peaks with respect to the expectd edge locations.

4. The Si K Edge in CCD Devices

From the emission properties shown in Table 2 it is concluded that these are effects caused by the HETG spectrometer. This is supported by the fact that these emission properties appear fairly independent of source column density and source flux. Furthermore these emissions are not observed in the raw (unbinned) MEG +1st orders which are recorded on a back-illuminated (BI) device, but only in orders that involve front-illuminated (FI) devices.

5. Si K Edge in FI CCDs

These are distinct differences between BI and FI devices. One major difference is that BI devices do not possess a gate structure at the illuminated side as do FI devices. This gate structure produces intrinsic absorption due to the presence of SiO_2.

5.1. Transmission Function as measured at Synchrotron

The transmission signature of the SiO_2 gate structure of FI devices has been measured at several synchrotron facilities during the AXAF ground calibration phase. The results are summarized in Prigozhin et al. (1997). The gate structure contains polysilicon, SiO_2, and silicon nitrate. It prodcuces a distinct absorption imprint as a sum of all these components.

This imprint is shown in Figure 5. The large step appear at a value we associate with atomic Si near 1.839 keV. There are two distinct absorption minima near 1.840 keV and

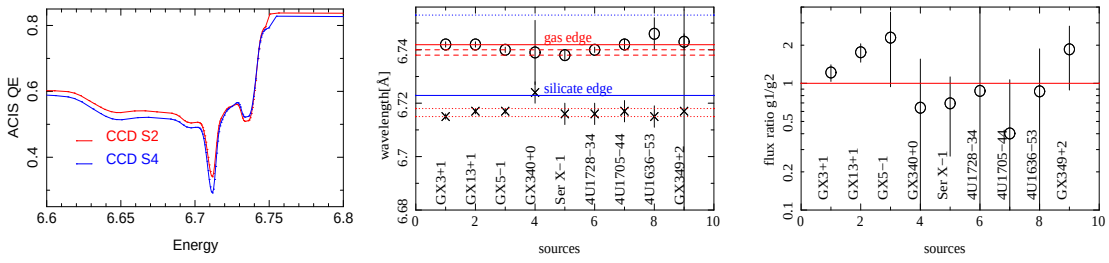

Fig. 4.— *Left:* The Si K edge structure as implemenated for S2 (red) and S4 (blue).

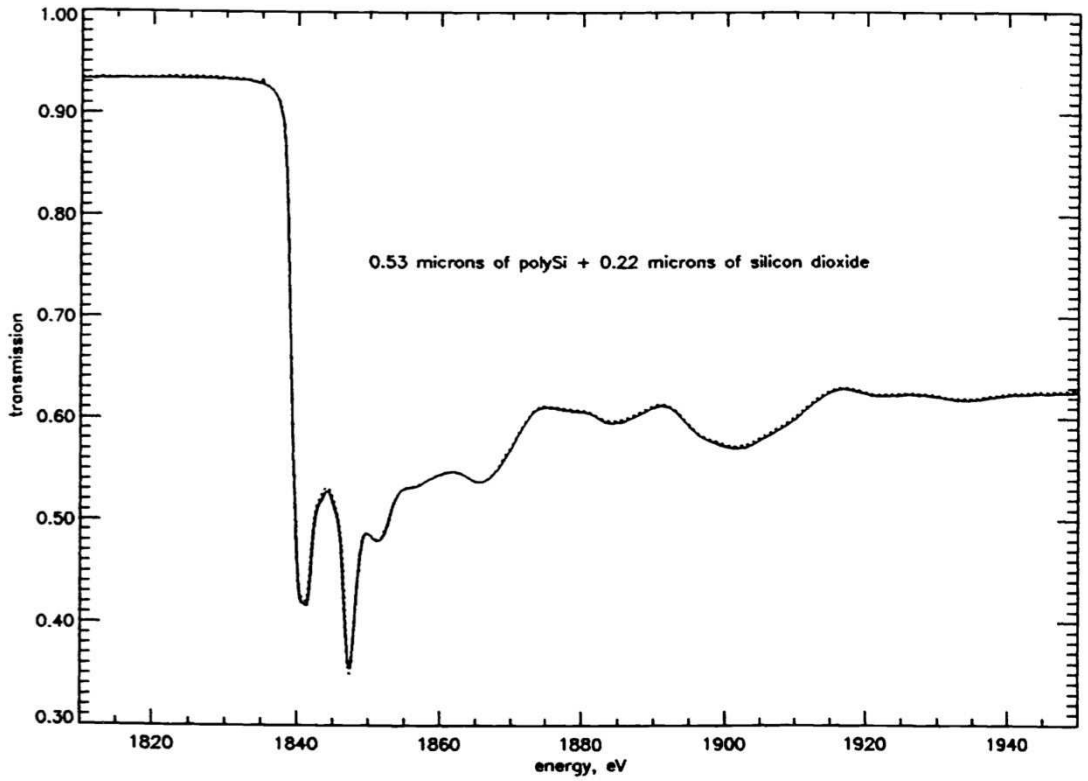

Fig. 5.— Transmission function as determined from fits to synchrotron measurments of combined oxidized polysilicon film and SiO_2 as found in the gate structure of FI CCDs (from Prigozhin et al. 1997).

1.846 keV and some weaker minima and higher energies. In middle plot of Figure 4 we highlight the locations of these minima with the dotted line regions. The closeness of these minima to the location where we observe the emissions as well as the fact that they are only observed in devices that possesses this gate structure absorption imprint makes it a good candidate for the appearance of these emissions in the HEG data.

5.2. Si K edge in S2 and S4

In the HETG spectrometer the Si K edges in first order dispersion fall on three different devices, HEG -1st and MEG -1st both fall on S2, MEG +1st order falls on S3, HEG +1st order on S4. The devices S2 and S4 were not directly measured at a synchrotron facility and here the measured high resolution transmission curve shown in Figure 5 were fitted into the medium resolution effective areas measured during subassembly at MIT. The areas of S2 and S4 are slightly different and thus the high resolution Si pattern also appears slightly different in these devices as shown in the left plot of Fig. 4. This can have some impact of the R_{line} ratios between data taken with different subarrays where at 350 rows the patterns of both S2 and S4 are co-added, while at 134 rows only S2 contributes.

6. Conclusions

Based on the properties of the faint line emissions in the Si K edge region, its sole appearance on FI devices, the fact that the line wavelengths coincide with the main absorption minima of the SiO_2 gate structure pattern we tentatively conclude that these emissions are caused by this pattern. Their properties in the data so far show that they are independent of source column density and source flux and thus likely instrumental. The effect is rather subtle, the line to continuum ratio is less than 1%, and appears most effective in unbinned (raw) data and very long exposures. This effect should not affect the bulk of any HETG spectral analyses. However, specifically in the case of detailed studies of the Si K edge structure of celestrial sources where mostly unbinned HEG data at long exposures are applied, it is relevant and need to be considered. We also conclude that for now the best recipe to model this effect in these cases is to add two unresolved (line σ ¡ 0.005 Å) Gaussian line functions at 6.717 Åand 6.742 Åto any model and constrain the R_{line} ratio to within a certain percentage of unity depending on statistics.

The latter procedure should be valid no matter if the SiO_2 gate structure pattern is the true cause of not. We are still collecting data specifically with respect of a possible long term

time variability. It is also unclear at this point what corrective action needs to be taken in future calibrationi efforts.

7. References

Marshall et al. 2012, SPIE Vol. 8443, 48
Prigozhin et al. 1998, SPIE Vol. 3301, p.108
Rogantini et al. 2010, 641, 149
Schulz et al. 2016, ApJ, 827, 49
Yang et al. 2022, ApJ, submitted
Zeegers et al. 2015, A&A, 2017, 599, 117a